

**Table 1.** List of compounds used in the present study.

Compound (abbreviation)	No. of mobilized genes (ANOVA, p<0.05)	Usage	Hepatotoxicity	Proposed toxicological action
alpha-naphthylisothiocyanate (ANIT)	1063	hepatotoxins	cholestasis	toxic metabolite can injure epithelial cells in biliary duct
amiodarone hydrochloride (AM)	640	antiarrhythmic, antianginal agents	phospholipidosis	oxidative stress by free radical
benzbromarone (BBr)	1720	uricosuric agents	hepatomegaly	peroxisome proliferators-like action
carbon tetrachloride (CCL4)	2262	hepatotoxins	hepatocellular carcinoma fatty liver	production of toxic metabolite that leads to peroxidative injury of membrane lipids and membrane perturbation
clofibrate (CFB)	1800	antilipemic agents	hypertrophy, hepatocellular carcinoma	peroxisome proliferator
coumarin (CMA)	1005	hepatotoxins	necrosis	formation of coumarin 3,4-epoxide
gemfibrozil (GFZ)	1943	antilipemic agents	hepatomegaly	peroxisome proliferator
isoniazid (INAH)	1482	antituberculous agents	necrosis	generation of a reactive metabolite from acetyldiazine
methapyrilene (MP)	4910	antiallergic, hypnotic, sedative agents	carcinoma	induction of hepatic cell proliferation, lipid peroxidation of the liver
omeprazole (OPZ)	1441	antiulcer agents	elevation of serum enzyme	unknown
Phenobarbital (PB)	548	hypnotics, sedatives, anticonvulsants	hepatocellular tumor	induction of c-fos gene expression
propylthiouracil (PTU)	1544	antithyroid agents	elevation of serum enzyme	thyroxin synthesis inhibitor
sulfasalazine (SS)	860	antiinflammatory, antirheumatic, antiinfective agents	genotoxicity, carcinogenicity	antiinflammatory, antibacterial actions, inhibition of production of cytokines
thioacetamide (TAA)	5712	hepatotoxins	carcinogenicity	hepatocarcinogen
Wy-14,643 (WY)	4307	hepatotoxins	carcinoma hepatomegaly	peroxisome proliferator

Gene expression in rat liver with triglyceride decreasing compounds.

manufacturer's instructions. Microarray analysis was conducted on 3 out of 5 samples for each group by using GeneChip® RAE 230A probe arrays (Affymetrix, Santa Clara, CA, USA), containing 15,923 probe sets. The procedure was conducted basically according to the manufacturer's instructions using Superscript Choice System (Invitrogen, Carlsbad, CA, USA) and T7-(dT)24-oligonucleotide primer (Affymetrix) for cDNA synthesis, cDNA Cleanup Module (Affymetrix) for purification, and BioArray High yield RNA Transcript Labeling Kit (Enzo Diagnostics, Farmingdale, NY, USA) for synthesis of biotin-labeled cRNA. Ten micrograms of fragmented cRNA was hybridized to a RAE230A probe array for 18 hr at 45°C at 60 rpm, after which the array was washed and stained by streptavidin-phycoerythrin using Fluidics Station 400 (Affymetrix) and scanned by Gene Array Scanner (Affymetrix). The digital image files were processed by Affymetrix Microarray Suite version 5.0. Microarray image data were analyzed with GeneChip Operating Software (Affymetrix).

#### Statistical analysis

Plasma TG and food consumption results were expressed as means  $\pm$  SD. They were analyzed by Bartlett test that evaluates the homogeneity of variance. If the variances were homogenous, ANOVA was applied. If the variances were heterogeneous, Kruskal-Wallis test was performed. When ANOVA resulted in a statistical difference between the groups, Dunnett test was applied. When Kruskal-Wallis test resulted in statistically different groups, Dunnett type mean rank test was performed. Identification of genes related to plasma TG decrease and gene expression data were analyzed by Welch ANOVA for the dose level and applied with Benjamini and Hochberg False Discovery Rate as a multiple-testing correction. In these tests, a significant level at  $p < 0.05$  was considered acceptable (Snedecor and Cochran, 1989).

GeneChip data were normalized by the global median normalization method using GeneSpring version 7 (Agilent Technologies Inc., Palo Alto, CA, USA). Probe sets with present or marginal call in at least 1 of 48 samples ( $N=3$  for 4 time points and 4 dose levels) were selected. Principal component analysis (PCA) of the GeneChip data was performed using Spotfire DecisionSite ver. 8.2 (Spotfire, Somerville, MA, USA).

#### Pathway and Gene Ontology (GO) analysis

The identified probe sets were subjected to anal-

ysis of Kyoto Encyclopedia of Genes and Genomes (KEGG) pathway and GO analysis by DAVID (Database for Annotation, Visualization, and Integrated Discovery; <http://apps1.niaid.nih.gov/david/>) using Fisher's exact test (Dennis *et al.*, 2003). Level 5 analysis was adopted.

## RESULTS

#### Plasma biochemistry and food consumption

Rats were treated with each compound (ANIT, AM, BBr, CCL4, CFB, CMA, GFZ, INAH, MP, OPZ, PB, PTU, SS, TAA and WY) by gavage for up to 4 weeks. The TG concentration and food consumption results are shown in Fig. 1. All compounds that we selected showed a TG-decreasing property during the dosing period, while their effects on food consumption differed. In BBr-, CMA-, OPZ- and SS-treated animals, food consumption transiently dropped in the first 3 days while it returned to normal thereafter. In AM-, INAH- and TAA-treated rats, food consumption was depressed throughout the dosing period. PTU-treatment decreased food consumption from day 15 whereas MP-treatment decreased at day 29. ANIT-, CFB-, CCL4, GFZ-, PB-, and WY-treatment affected the food intake only slightly.

#### Identification of genes related to the plasma TG-decreasing property

After filtering the probe sets (with present or marginal call in at least 1 of 48 samples), Welch ANOVA with multiple testing correction was applied to each compound to extract significantly mobilized probe sets. As shown in Table 1, the numbers of extracted probe sets varied among the compounds, from 640 (AM) to 5,712 (TAA). We then selected the probe sets that were commonly changed from more than 10 out of 15 compounds, and 218 probe sets were obtained. KEGG pathway analysis revealed that pathways related to "proteasome", "fatty acid metabolism", "amino acid metabolism", and "bile acid biosynthesis" were mainly altered in liver treated with these compounds (Table 2). GO analysis showed that some groups (other than cellular lipid metabolism) related to xenobiotics metabolism, such as carboxylic acid metabolism, and glucuronosyltransferase and aldehyde dehydrogenase activity, were also affected in liver (Table 3).

#### Principal component analysis (PCA)

To assess the expression profiles of identified

## Gene expression in rat liver with triglyceride decreasing compounds.

probe sets, PCA with 218 probe sets for data of all 15 compounds were performed. As shown in Fig. 2, each sample was separated from control according to the expression of these probe sets. Each sample tended to have a smaller value in the component PC 1 as the treatment period increased, and each was distinctly separated into either direction in component PC 2. It should be noted that liver treated with WY, BBr, GFZ and CFB had a relatively large principal component PC 2, while PTU, OPZ, PB, TAA, MP, SS and CMA showed small PC 2. Liver treated with AM for 28 days had a near zero value in PC 2. Some compounds such as ANIT, CCL4 and INAH did not change their position very much.

To elucidate which genes contributed more for

each principal component, eigenvector values of each probe sets were examined. As shown in Table 4, “vanin 1”, “similar to Aig1 protein”, “CD36 antigen”, and “cell death-inducing DNA fragmentation factor, alpha subunit-like effector A” had large eigenvector values for PC 2. Meanwhile, “glutathione *S*-transferase A5, aldehyde dehydrogenase family 1, member A1”, “liver UDP-glucuronosyltransferase, phenobarbital-inducible form”, “carbonic anhydrase 2” and “cytochrome P450, family 2, subfamily b, polypeptide 15” had small values for PC 2 (Table 5). “Aldehyde dehydrogenase family 1, member A1”, “glutathione *S*-transferase A5”, “vanin 1”, “carboxylesterase 2 (intestine, liver)” and “CD36 antigen” had smaller eigenvector values for PC 1 (Table 6).

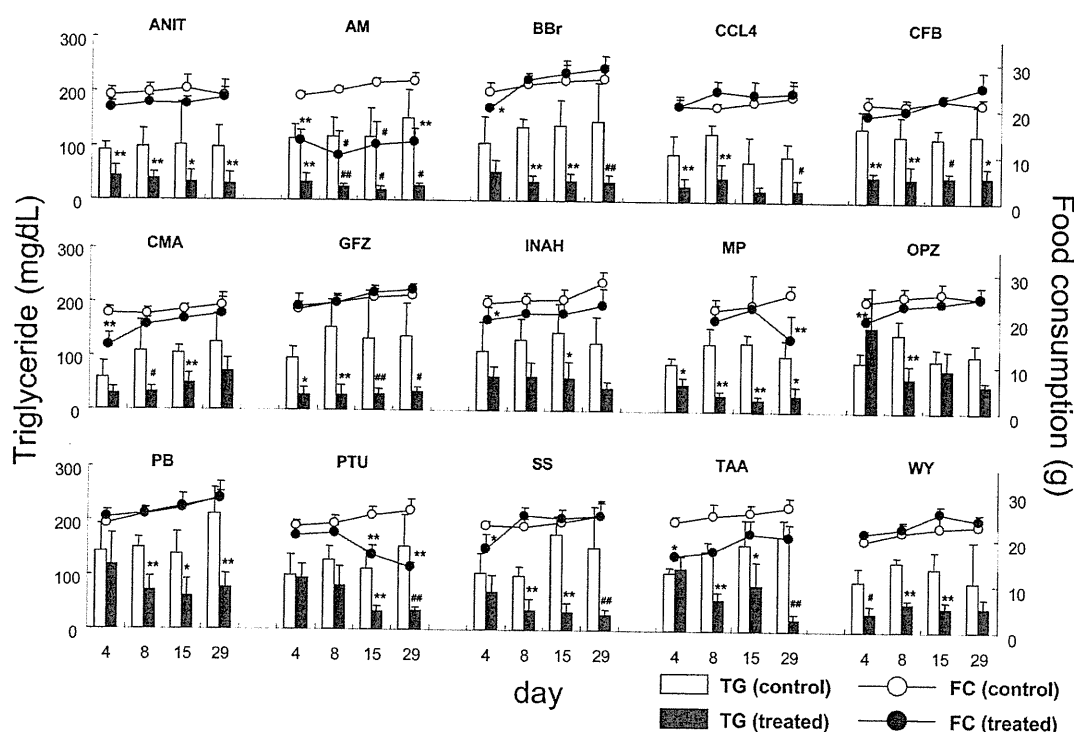


**Fig. 1.** Effects of TG-decreasing compounds on food consumption and plasma TG level.

Six-week-old male Sprague-Dawley rats were gavaged with each compound for 3, 7, 14 or 28 days, and they were sacrificed 24 hr after the last dosing. Food consumption was recorded every 4 days during dosing and blood samples were collected at sacrifice. Plasma TG concentrations were estimated as described in materials and methods. For simplicity, the data of the highest dose were presented for each compound. Open (control) and filled (treated) columns represent plasma TG concentration. Open (control) and filled (treated) circles represent food consumption. Values are expressed as mean  $\pm$  SD of 5 rats each for each time and compound. Significant difference from control rat: (\* $p$ <0.05, \*\* $p$ <0.01: Dunnett test, # $p$ <0.05, ## $p$ <0.01: Dunnett type mean rank test). MP-food consumption on day 4 was not determined.

As PC 2 was considered to be indirectly related to cholesterol metabolism (see DISCUSSION), three compounds with the smallest values for both PC 1 and PC 2, i.e., PB, OPZ and PTU were selected, and their effects on plasma cholesterol level are shown in Fig. 3. It is obvious from the figure that OPZ and PTU, which had smaller PC 2 values than PB, significantly increased plasma cholesterol.

## DISCUSSION

Lowering of the plasma TG level is often observed in rat toxicity studies. It would be useful to elucidate its mechanism not only for safety evaluation of drugs but also for finding seeds of lipid-lowering agents. In the course of our trials to identify useful toxicity biomarkers from our large-scale database, we selected plasma TG decrease as a toxicological phenotype, and picked up 15 such compounds from 40 (the number of compounds available at the time when the

**Table 2.** KEGG pathways of the identified 218 probe sets related to plasma TG.

Term	Count	p value
proteasome	8	1.66E-06
fatty acid metabolism	10	4.61E-06
tryptophan metabolism	9	3.44E-05
bile acid biosynthesis	4	0.00997
histidine metabolism	4	0.00997
propanoate metabolism	4	0.0224
fatty acid biosynthesis (path 2)	3	0.0236
pyruvate metabolism	4	0.0289
valine, leucine and isoleucine degradation	4	0.0289
nitrogen metabolism	3	0.0364
arginine and proline metabolism	4	0.0492

Statistically extracted 218 probe sets related to plasma TG were categorized by KEGG pathway. The terms with significantly high counts (Fisher's exact test;  $p < 0.05$ , calculated by DAVID: <http://apps1.niaid.nih.gov/david/>) are presented in the table.

**Table 3.** Gene ontology of the identified 218 probe sets related to plasma TG.

Category	Term	Counts	p value
Biological process	carboxylic acid metabolism	15	5.25E-06
	electron transport	14	1.83E-04
	fatty acid metabolism	8	6.04E-04
	response to chemical substance	7	0.00164
	cellular lipid metabolism	10	0.0115
	amino acid metabolism	6	0.0154
	protein catabolism	11	0.0492
Molecular function	glucuronosyltransferase activity	6	5.01E-05
	aldehyde dehydrogenase activity	3	0.0249
Cellular component	endoplasmic reticulum	15	1.25E-05
	microsome	9	1.93E-04
	microrbody	5	0.00726
	peroxisome	5	0.00726
	proteasome complex (SENSU EUKARYOTA)	4	0.00829
	proteasome core complex (SENSU EUKARYOTA)	4	0.00829
	mitochondrion	15	0.0103

Statistically extracted 218 probe sets related to plasma TG were categorized by gene ontology. The terms with significantly high counts (Fisher's exact test;  $p < 0.05$ , calculated by DAVID: <http://apps1.niaid.nih.gov/david/>) are presented in the table.

## Gene expression in rat liver with triglyceride decreasing compounds.

present analysis was performed). Since our database has a broad variety of compounds for hepatic toxicity, each compound has different properties for drug efficacy and toxicity (Table 1).

As shown in Fig. 1, the effects of these compounds on food consumption were not similar. It is well known that plasma TG levels depend largely upon nutrition, and the results suggested that there should have been multiple factors other than a simple general toxicity. To clarify the multiple mechanisms in plasma TG homeostasis, we extracted 218 probe sets as com-

monly changed genes in more than 10 out of 15 compounds (commonly changed in two-thirds of the compounds). The fact that there were no probe sets commonly changed in all the compounds (data not shown) also suggested that there are multiple factors involved in the mechanism of plasma TG decrease.

KEGG pathway analysis suggested that the proteasome-, fatty acid metabolism-, tryptophan metabolism-, bile acid biosynthesis-, and histidine metabolism-related pathways were involved (Table 2). Since TG is an important source of energy, it is understood

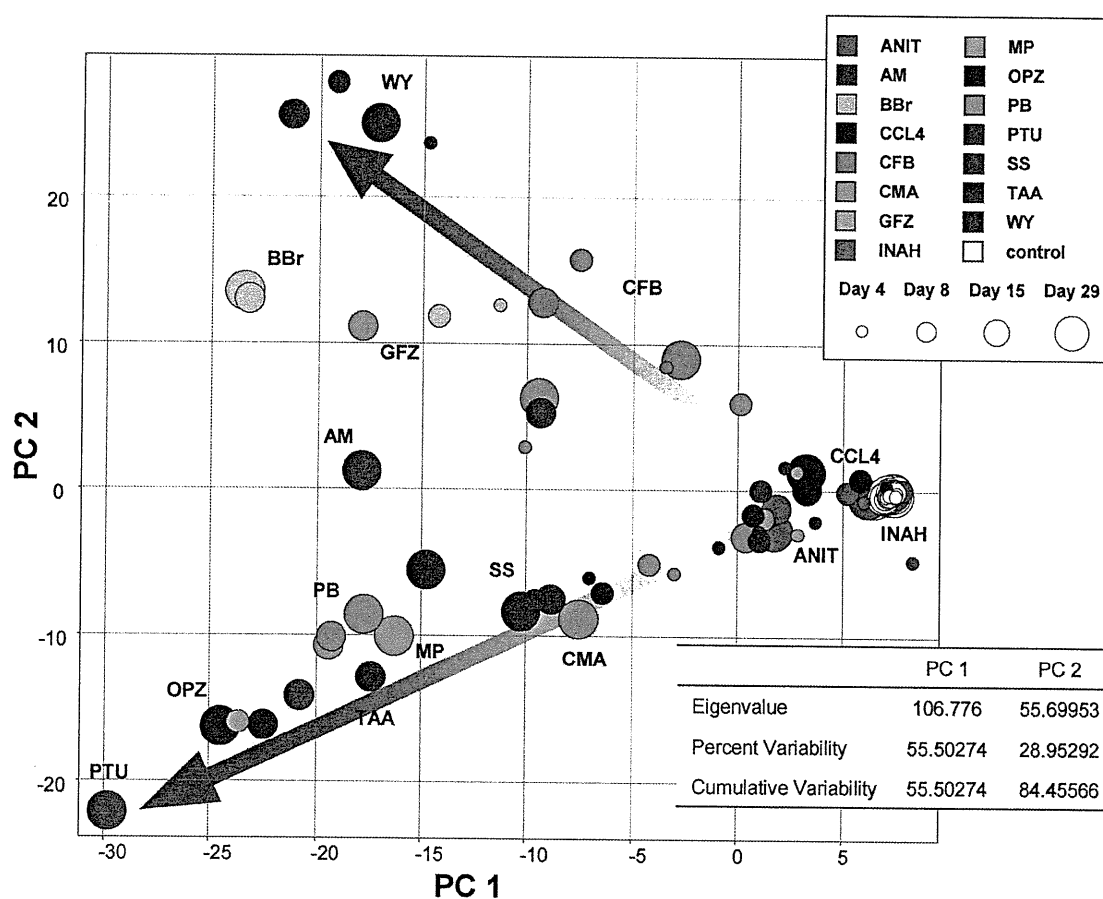


Fig. 2. Principal component analysis of gene expression profiles.

PCA of gene expression profiles was performed using identified 218 probe sets for the data of the highest dose of 15 compounds at various time points. The selection of the 218 probe sets related to plasma TG decrease is described in materials and methods. The values used in the analysis were the normalized signal values. Each spot represents the mean of the normalized gene expression value. The abbreviation for each drug is summarized in Table 1. The eigenvalue, percent variability, and cumulative variability for PC 1 and PC 2 are shown in the table on the lower right corner.

that pathways related to energy homeostasis such as fatty acid synthesis and amino acid metabolism were affected. GO analysis showed that the carboxylic acid metabolism- and glucuronosyltransferase activity-related genes were also affected by TG-decreasing compounds (Table 3). UDP-glucuronosyltransferase, one of the extracted genes, is of major importance in conjugation and subsequent elimination of potentially toxic xenobiotics (Bock *et al.*, 1990). PB and OPZ, which lowered plasma TG level in the present study, were previously reported to have the ability to induce this enzyme (Bock *et al.*, 1990; Masubuchi *et al.*, 1997). These results indicated that the xenobiotics metabolism pathway might have a role in plasma TG decrease.

To examine the basis of the gene expression pro-

file of each sample, we performed PCA on hepatic gene expression profiles of the 15 compounds. In PCA, three clear clusters were identified (Fig. 2). All compounds except ANIT, CCL4 and INAH were uniformly dispersed into smaller PC 1 with either large or small PC 2, i.e., WY, BBr, GFZ and CFB were dispersed into small PC 1 with large PC 2, whereas PTU, OPZ, PB,MP, TAA, SS and CMA into small PC 1 with small PC 2. AM was exceptionally found in the middle position of PC 2.

In PC 2, “vanin 1”, “similar to Aig1 protein”, “CD36 antigen”, “cell death-inducing DNA fragmentation factor, and alpha subunit-like effector A (CIDEA)” had larger eigenvector values (Table 4), meaning that these genes made a great contribution to increasing PC 2 values in each liver sample. Vanin 1 is

**Table 4.** Top five probe sets with the largest eigenvector values for second principal component in the PCA shown in Fig. 2.

Ranking	Probe ID	PC 2	Description
1	1389253_at	0.610	Vanin 1 (predicted)
2	1375845_at	0.291	Similar to Aig1 protein
3	1367689_a_at	0.230	CD36 antigen
4	1389179_at	0.180	Cell death-inducing DNA fragmentation factor, alpha subunit-like effector A (predicted)
5	1386901_at	0.153	CD36 antigen

Each eigenvector value was calculated by Spotfire DecisionSite.

**Table 5.** Top five probe sets with the smallest eigenvector values for second principal component in the PCA shown in Fig. 2.

Ranking	Probe ID	PC 2	Description
1	1371089_at	-0.526	Glutathione <i>S</i> -transferase A5
2	1387022_at	-0.187	Aldehyde dehydrogenase family 1, member A1
3	1370698_at	-0.113	Liver UDP-glucuronosyltransferase, phenobarbital-inducible form
4	1386922_at	-0.0742	Carbonic anhydrase 2
5	1371076_at	-0.0586	Cytochrome P450, family 2, subfamily b, polypeptide 15

Each eigenvector value was calculated by Spotfire DecisionSite.

**Table 6.** Top five probe sets with the smallest eigenvector values for first principal component in the PCA shown in Fig. 2.

Ranking	Probe ID	PC 1	Description
1	1387022_at	-0.630	Aldehyde dehydrogenase family 1, member A1
2	1371089_at	-0.491	Glutathione <i>S</i> -transferase A5
3	1389253_at	-0.370	Vanin 1 (predicted)
4	1368905_at	-0.163	Carboxylesterase 2 (intestine, liver)
5	1367689_a_at	-0.162	CD36 antigen

Each eigenvector value was calculated by Spotfire DecisionSite.

## Gene expression in rat liver with triglyceride decreasing compounds.

reported to be involved in lymphocyte migration in cell adhesion during colonization of the thymus by hematopoietic precursor cells, and also has pantetheinase activity (Pitari *et al.*, 2000). Though vanin 1 is not reported to play a role in lipid metabolism so far, it was in fact reported to be an inducible gene by PPAR $\alpha$  (Yamazaki *et al.*, 2002).

CD36 antigen (fatty acid translocase (FAT)) is involved in regulating the uptake of fatty acid across the plasma membrane (Bonen *et al.*, 2004) and also reported to be induced by PPAR $\alpha$  agonists in liver (Motojima *et al.*, 1998). Moreover, it has been reported that CD36 plays a role in plasma TG homeostasis via modulation of LPL activity (Goudriaan *et al.*, 2005). Thus, an increase of this gene expression would be one of the mechanisms of plasma TG level decrease in the corresponding animal.

A previous report described that CIDEA-null mice presented TG decrease in fasting condition compared with wild type (Zhou *et al.*, 2003). Because expression of the CIDEA gene was up-regulated in liver treated with TG-decreasing compounds in both principal components (data not shown), it seemed to be a compensatory reaction. In addition, compounds with large PC 2 values, i.e., WY, GFZ, CFB and BB<sub>r</sub>, are

reported to be agonists of PPAR $\alpha$  (Kunishima *et al.*, 2003; van Raalte *et al.*, 2004). Activation of PPAR $\alpha$  induces hepatic gene expression by  $\beta$ -oxidation of fatty acid and hydrolysis of TG-rich lipoprotein via activation of peripheral lipoprotein lipase (LPL) (van Raalte *et al.*, 2004). In addition to activation of fatty acid  $\beta$ -oxidation, PPAR $\alpha$  inhibits de novo fatty acid synthesis in liver (Schoonjans *et al.*, 1996). In peripheral tissue, it has also been reported that gene expression of APOC3 (a natural inhibitor of LPL activity) decreases by PPAR $\alpha$  and subsequently LPL activity is increased (Staels *et al.*, 1995). Taken together, these results suggest that the trend of increasing PC 2 is linked to lowering plasma TG level via PPAR $\alpha$  activation.

“Glutathione S-transferase A5”, “aldehyde dehydrogenase family 1, member A1”, “liver UDP-glucuronosyltransferase, phenobarbital-inducible form”, “carbonic anhydrase 2”, “cytochrome P450, family 2, subfamily b, polypeptide 15” had smaller eigenvector values for PC 2 (Table 5). They (except carbonic anhydrase 2) have been reported to be constitutive androstane receptor (CAR)-inducible genes (Kakizaki *et al.*, 2003). Although there is no report that PTU, OPZ, TAA, MP, SS and CMA activate CAR so far, the present results suggested that these compounds could

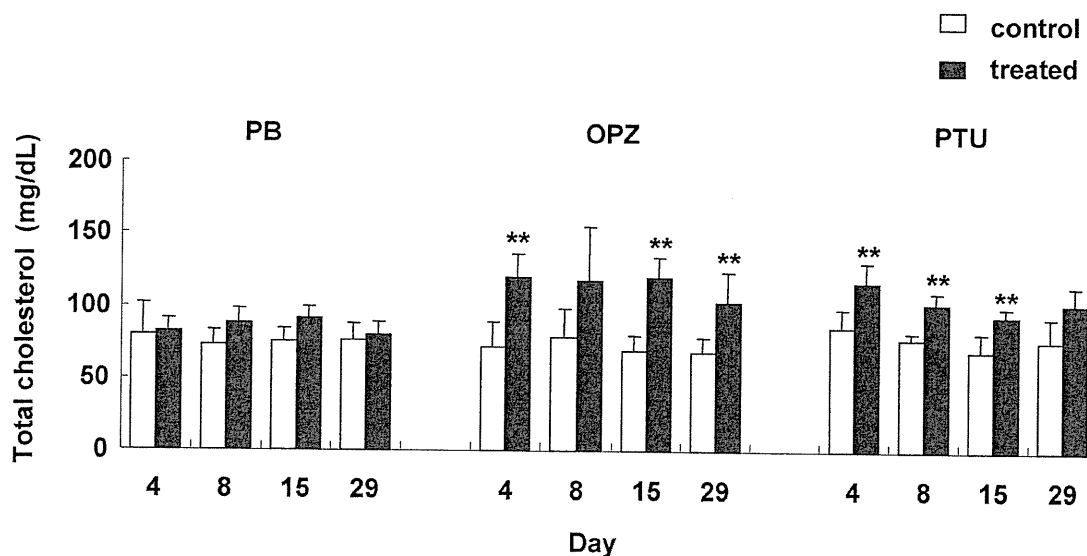


**Fig. 3.** Effects of PB, OPZ, PTU on plasma total cholesterol level. Plasma total cholesterol concentrations were estimated as described in materials and methods. Open (control) and filled (treated) columns represent total plasma cholesterol concentration. Values are expressed as mean  $\pm$  SD of 5 rats for each time and compound. Significant difference from control rat: (\* $p$ <0.05, \*\* $p$ <0.01; Dunnett test).

induce the same xenobiotics metabolizing enzymes as PB does (Kakizaki *et al.*, 2003). Meanwhile, these enzymes (such as UDP-glucuronosyltransferase) are able to metabolize not only xenobiotics but also serum thyroid hormone (TH) (Qatanani and Moore, 2005), which has a role in comprehensive regulation of energy metabolism (Weiss *et al.*, 1998). It has been reported that rats with hypothyroidism induce and activate peripheral lipoprotein lipase (LPL), the key enzyme in hydrolysis of TG-rich lipoproteins, such as chylomicron and VLDL (Kern *et al.*, 1996; Ong *et al.*, 1994). In fact, it has also been reported that PB, PTU and OPZ are able to alter blood TH level (Masubuchi *et al.*, 1997; De Sandro *et al.*, 1991). CAR is also activated by caloric restriction (Maglich *et al.*, 2004). With depletion of food, the body needs to lower its energy requirement. It might be possible that CAR was activated in rats whose food consumption was decreased (Fig. 1). Thus, identified probe sets might be indirectly related to plasma TG decrease via reduction of blood TH by CAR activation in at least two ways. Accordingly, the feature in decreased PC 2 value could be related to lowering plasma TG level via CAR activation. Moreover, it has been reported that TH is a physiological regulator of cholesterol metabolism (Weiss *et al.*, 1998; Gullberg *et al.*, 2000, 2002; Hashimoto *et al.*, 2006; Ness and Chambers, 2000) and hypercholesterolemia is found in patients with hypothyroidism (Diekman *et al.*, 2000). It was also noted in the present study that total cholesterol levels in OPZ and PTU with smaller PC 2 values were found to be increased (Fig. 3). These indirect evidences also supported the assumption that TH levels were involved in plasma TG reduction.

As shown in Table 6, genes with smaller eigenvector values for PC 1 such as "aldehyde dehydrogenase A5", "glutathione S-transferase A5", "vanin 1", "carboxylesterase 2" and "CD36 antigen" were important genes that contribute to shift each sample to either direction of PC 2. It appears that PC 1 shows a lowering of plasma TG level via either or both of two mechanisms (PPAR $\alpha$  and/or CAR activation). Interestingly, AM had small PC 1 values, while near zero in PC 2. This result is supported by previous reports that AM induces the expression of PPAR $\alpha$  target genes (McCarthy *et al.*, 2004) and lowers serum TH level (De Sandro *et al.*, 1991). Thus, these two directions might have been balanced in the case of the plasma TG reduction by AM.

It was previously reported that PPAR $\alpha$  was also activated by fasting (Kersten *et al.*, 1999; Lee *et al.*,

2004; Leone *et al.*, 1999), as well as by CAR. An interesting question is why these 218 probe sets classify the compounds with various pharmacological and toxicological properties based on their different mechanisms. Genes with the largest or smallest eigenvector values for PC 2 such as vanin 1 and glutathione S-transferase A5 are related to each nuclear receptor, PPAR $\alpha$  and CAR, respectively, rather than to plasma TG homeostasis. CD36, which was involved in regulating the uptake of fatty acid, mainly contributed to PC 1. This means that CD36 could be an important gene directly related to plasma TG level, while its background mechanisms are represented by genes like vanin 1 or glutathione S-transferase A5. Thus, we considered that these probe sets work to classify the compounds by PCA, based on each nuclear receptor-mediated TG-lowering mechanism.

In the present study, some compounds such as ANIT, CCL4 and INAH were not dispersed in PCA, suggesting potential involvement of other TG-decreasing mechanism(s). Because the plasma TG level is influenced by the balance of intake from diet, hepatic synthesis, secretion from liver, and metabolism at peripheral tissues, many factors remain to be investigated. Moreover, since it has been reported that the action of TH on LPL activity is in the opposite direction between human and rat (Kern *et al.*, 1996; Ong *et al.*, 1994), it is necessary to elucidate the species difference in the mechanism of plasma TG decrease.

In conclusion, we identified 218 probe sets from gene expression profiles in liver treated with various TG-decreasing compounds stored in our database. Analysis of identified probe sets suggested two mechanisms in plasma TG decrease, i.e., PPAR $\alpha$  and CAR activation, in addition to at least one unknown mechanism. The proposed mechanisms of lowering plasma TG level elucidated by the present study are summarized and depicted in Fig. 4. Further studies, especially verifying experiments, are clearly necessary to confirm our hypothesis and to establish useful biomarker genes. The presently extracted probe sets could be a source of potential biomarkers for development of a novel hypolipidemic agent and/or interpretation of the mechanism of plasma TG reduction.

#### ACKNOWLEDGMENT

We thank Nami Asari, Seiko Ueda, Chiaki Kondo, Shogo Hayakawa, Yasunori Suzuki, Izumi Yumita, Hayato Fukusumi and Seiko Ohta (Toxicogenomics Project in Japan) for analyses of liver gene



## Gene expression in rat liver with triglyceride decreasing compounds.

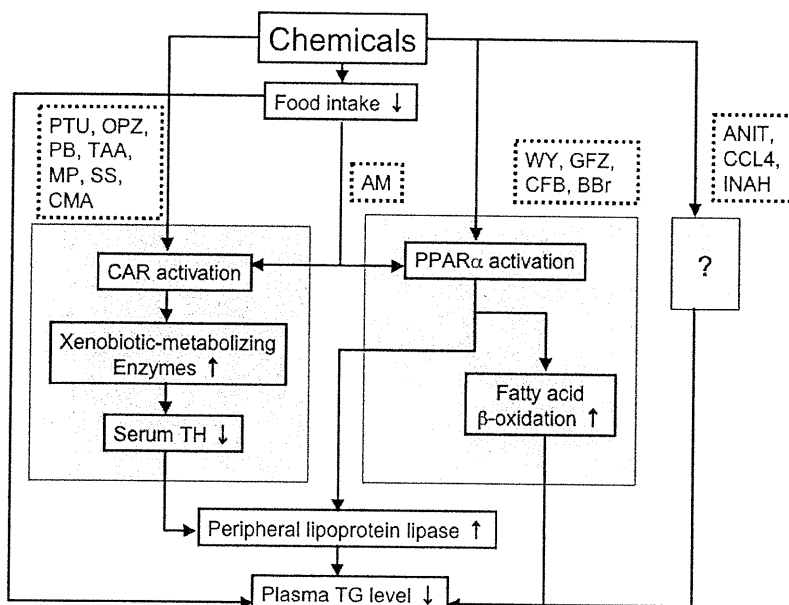


Fig. 4. Proposed TG-decreasing mechanisms of various drugs elucidated by comprehensive gene expression analysis.

Intake of chemicals induces direct or indirect CAR and/or PPAR $\alpha$  activation. CAR activation leads to induction of hepatic xenobiotic-metabolizing enzymes, which reduces the serum thyroid hormone (TH) level. PPAR $\alpha$  activation leads to hepatic induction of fatty acid  $\beta$ -oxidation. Both of the nuclear receptor activations increase peripheral lipoprotein lipase activity, which subsequently lowers the plasma TG level. PTU, OPZ, PB, TAA, MP, SS, and CMA are CAR activators, whereas WY, GFZ, CFB, and BBr are PPAR $\alpha$  activators. AM appears to have both properties to the same extent. There must be other mechanism(s), since ANIT, CCL4, and INAH, which showed obvious TG-decreasing effects, could not be differentiated by the present analysis.

expression. This study was supported in part by a grant from the Ministry of Health, Labor and Welfare (H14-Toxico-001).

## REFERENCES

- Bock, K.W., Lipp, H.P. and Bock-Hennig, B.S. (1990): Induction of drug-metabolizing enzymes by xenobiotics. *Xenobiotica*, **20**, 1101-1111.
- Bonen, A., Campbell, S.E., Benton, C.R., Chabowski, A., Coort, S.L., Han, X.X., Koonen, D.P., Glatz, J.F. and Luiken, J.J. (2004): Regulation of fatty acid transport by fatty acid translocase/CD36. *Proc. Nutr. Soc.*, **63**, 245-249.
- Dennis, G. Jr., Sherman, B.T., Hosack, D.A., Yang, J., Gao, W., Lane, H.C. and Lempicki, R.A. (2003): DAVID: Database for annotation, visualization, and integrated discovery. *Genome Biol.*, **4**, 3.
- De Sandro, V., Chevrier, M., Boddaert, A., Melcion, C., Cordier, A. and Richert, L. (1991): Comparison of the effects of propylthiouracil, amiodarone, diphenylhydantoin, phenobarbital, and 3-methylcholanthrene on hepatic and renal T4 metabolism and thyroid gland function in rats. *Toxicol. Appl. Pharmacol.*, **111**, 263-278.
- Diekman, M.J., Angheliescu, N., Endert, E., Bakker, O. and Wiersinga, W.M. (2000): Changes in plasma low-density lipoprotein (LDL)- and high-density lipoprotein cholesterol in hypo- and hyperthyroid patients are related to changes in free thyroxine, not to polymorphisms in LDL

- receptor or cholesterol ester transfer protein genes. *J. Clin. Endocrinol. Metab.*, **85**, 1857-1862.
- Goudriaan, J.R., den Boer, M.A., Rensen, P.C., Febbraio, M., Kuipers, F., Romijn, J.A., Havekes, L.M. and Voshol, P.J. (2005): CD36 deficiency in mice impairs lipoprotein lipase-mediated triglyceride clearance. *J. Lipid Res.*, **46**, 2175-2181.
- Gullberg, H., Rudling, M., Forrest, D., Angelin, B. and Vennstrom, B. (2000): Thyroid hormone receptor beta-deficient mice show complete loss of the normal cholesterol 7 $\alpha$ -hydroxylase (CYP7A) response to thyroid hormone but display enhanced resistance to dietary cholesterol. *Mol. Endocrinol.*, **14**, 1739-1749.
- Gullberg, H., Rudling, M., Salto, C., Forrest, D., Angelin, B. and Vennstrom, B. (2002): Requirement for thyroid hormone receptor beta in T3 regulation of cholesterol metabolism in mice. *Mol. Endocrinol.*, **16**, 1767-1777.
- Hall, I.H., Patrick, M.A. and Maguire, J.H. (1990): Hypolipidemic activity in rodents of phenobarbital and related derivatives. *Arch. Pharmacol.*, **323**, 579-586.
- Hashimoto, K., Cohen, R.N., Yamada, M., Markan, K.R., Monden, T., Satoh, T., Mori, M. and Wondisford, F.E. (2006): Cross-talk between thyroid hormone receptor and liver X receptor regulatory pathways is revealed in a thyroid hormone resistance mouse model. *J. Biol. Chem.*, **281**, 295-302.
- Hibbs, K., Skubitz, K.M., Pambuccian, S.E., Casey, R.C., Burleson, K.M., Oegema, Jr. T.R., Thiele, J.J., Grindle, S.M., Bliss, R.L. and Skubitz, A.P.N. (2004): Differential gene expression in ovarian carcinoma. Identification of potential biomarkers. *Am. J. Pathol.*, **165**, 397-414.
- Kakizaki, S., Yamamoto, Y., Ueda, A., Moore, R., Sueyoshi, T. and Negishi, M. (2003): Phenobarbital induction of drug/steroid-metabolizing enzymes and nuclear receptor CAR. *Biochim. Biophys. Acta*, **1619**, 239-242.
- Kern, P.A., Ranganathan, G., Yukht, A., Ong, J.M. and Davis, R.C. (1996): Translational regulation of lipoprotein lipase by thyroid hormone is via a cytoplasmic repressor that interacts with the 3' untranslated region. *J. Lipid Res.*, **37**, 2332-2340.
- Kersten, S., Seydoux, J., Peters, J.M., Gonzalez, F.J., Desvergne, B. and Wahli, W. (1999): Peroxisome proliferator-activated receptor alpha mediates the adaptive response to fasting. *J. Clin. Invest.*, **103**, 1489-1498.
- Kiyosawa, N., Tanaka, K., Hirao, J., Ito, K., Niino, N., Sakuma, K., Kanbori, M., Yamoto, T., Manabe, S. and Matsunuma, N. (2004): Molecular mechanism investigation of phenobarbital-induced serum cholesterol elevation in rat livers by microarray analysis. *Arch. Toxicol.*, **78**, 435-442.
- Kunishima, C., Inoue, I., Oikawa, T. and Katayama, S. (2003): The metabolism, toxicity and pharmacological studies of benzbromarone (Urinorm®). *J. Saitama Med. School*, **30**, 187-194.
- Lee, S.S., Chan, W.Y., Lo, C.K., Wan, D.C., Tsang, D.S. and Cheung, W.T. (2004): Requirement of PPARalpha in maintaining phospholipid and triacylglycerol homeostasis during energy deprivation. *J. Lipid Res.*, **45**, 2025-2037.
- Leone, T.C., Weinheimer, C.J. and Kelly, D.P. (1999): A critical role for the peroxisome proliferator-activated receptor alpha (PPARalpha) in the cellular fasting response: The PPARalpha-null mouse as a model of fatty acid oxidation disorders. *Proc. Nat. Acad. Sci. USA*, **96**, 7473-7478.
- Maglich, J.M., Watson, J., McMillen, P.J., Goodwin, B., Willson, T.M. and Moore, J.T. (2004): The nuclear receptor CAR is a regulator of thyroid hormone metabolism during caloric restriction. *J. Biol. Chem.*, **279**, 19832-19838.
- Masubuchi, N., Hakusui, H. and Okazaki, O. (1997): Effects of proton pump inhibitors on thyroid hormone metabolism in rats: A comparison of UDP-glucuronyltransferase induction. *Biochem. Pharmacol.*, **54**, 1225-1231.
- McCarthy, T.C., Pollak, P.T., Hanniman, E.A. and Sinal, C.J. (2004): Disruption of hepatic lipid homeostasis in mice after amiodarone treatment is associated with peroxisome proliferator-activated receptor-alpha target gene activation. *J. Pharm. Exp. Ther.*, **311**, 864-873.
- Motojima, K., Passilly, P., Peters, J.M., Gonzalez, F.J. and Latruffe, N. (1998): Expression of putative fatty acid transporter genes are regulated by peroxisome proliferator-activated receptor alpha and gamma activators in a tissue- and inducer-specific manner. *J. Biol. Chem.*, **273**, 16710-16714.
- Mutlib, A., Joang, P., Antherton, J., Obert, L., Kostrubsky, S., Madore, S. and Nelson, S. (2006): Identification of potential genomic biomarkers.

## Gene expression in rat liver with triglyceride decreasing compounds.

- arkers of hepatotoxicity caused by reactive metabolites of *N*-methylformamide: Application of stable isotope labeled compounds in toxicogenomic studies. *Chem. Res. Toxicol.*, **19**, 1270-1283.
- Ness, G.C. and Chambers, C.M. (2000): Feedback and hormonal regulation of hepatic 3-hydroxy-3-methylglutaryl coenzyme A reductase: The concept of cholesterol buffering capacity. *Proc. Soc. Exp. Biol. Med.*, **224**, 8-19.
- Ong, J.M., Simsolo, R.B., Saghizadeh, M., Pauer, A. and Kern, P.A. (1994): Expression of lipoprotein lipase in rat muscle: Regulation by feeding and hypothyroidism. *J. Lipid Res.*, **35**, 1542-1551.
- Pitari, G., Malergue, F., Martin, F., Philippe, J.M., Massucci, M.T., Chabret, C., Maras, B., Dupre, S., Naquet, P. and Galland, F. (2000): Pantetheinase activity of membrane-bound Vanin-1: Lack of free cysteamine in tissues of Vanin-1 deficient mice. *FEBS Lett.*, **483**, 149-154.
- Qatanani, M. and Moore, D.D. (2005): CAR, the continuously advancing receptor, in drug metabolism and disease. *Curr. Drug Metab.*, **6**, 329-339.
- Schoonjans, K., Staels, B. and Auwerx, J. (1996): Role of the peroxisome proliferator-activated receptor (PPAR) in mediating the effects of fibrates and fatty acids on gene expression. *J. Lipid Res.*, **37**, 907-925.
- Snedecor, G.W. and Cochran, W.G. (1989): *Statistical Methods*, 8th ed., Iowa State University Press.
- Staels, B., Vu-Dac, N., Kosykh, V.A., Saladin, R., Fruchart, J.C., Dallongeville, J. and Auwerx, J. (1995): Fibrates downregulate apolipoprotein C-III expression independent of induction of peroxisomal acyl coenzyme A oxidase. A potential mechanism for the hypolipidemic action of fibrates. *J. Clin. Invest.*, **95**, 705-712.
- Tan, Y., Shi, L., Hussain, S.M., Xu, J., Tong, W., Frazier, J.M. and Wang, C. (2006): Integrating time-course microarray gene expression profiles with cytotoxicity for identification of biomarkers in primary rat hepatocytes exposed to cadmium. *Bioinformatics*, **22**, 77-87.
- Urushidani, T. and Nagao, T. (2005): Toxicogenomics: The Japanese initiative. In (Borlak, J., ed.), *Handbook of Toxicogenomics - Strategies and Applications*, Wiley - VCH, pp. 623-631.
- van Raalte, D.H., Li, M., Pritchard, P.H. and Wasan, K.M. (2004): Peroxisome proliferator-activated receptor (PPAR)-alpha: A pharmacological target with a promising future. *Pharmaceut. Res.*, **21**, 1531-1538.
- Weiss, R.E., Murata, Y., Cua, K., Hayashi, Y., Seo, H. and Refetoff, S. (1998): Thyroid hormone action on liver, heart, and energy expenditure in thyroid hormone receptor beta-deficient mice. *Endocrinol.*, **139**, 4945-4952.
- Yamazaki, K., Kuromitsu, J. and Tanaka, I. (2002): Microarray analysis of gene expression changes in mouse liver induced by peroxisome proliferator-activated receptor alpha agonists. *Biochem. Biophys. Res. Comm.*, **290**, 1114-1122.
- Zhou, Z., Yon, T.-S., Chen, Z., Guo, K., Ng, C.P., Ponniah, S., Lin, S.C., Hong, W. and Li, P. (2003): Cidea-deficient mice have lean phenotype and are resistant to obesity. *Nat. Genet.*, **35**, 49-56.

## IDENTIFICATION OF GLUTATHIONE DEPLETION-RESPONSIVE GENES USING PHORONE-TREATED RAT LIVER

Naoki KIYOSAWA<sup>1</sup>, Takeki UEHARA<sup>1</sup>, Weihua GAO<sup>1</sup>, Ko OMURA<sup>1</sup>, Mitsuhiro HIRODE<sup>1</sup>,  
Toshinobu SHIMIZU<sup>1</sup>, Yumiko MIZUKAWA<sup>1,2</sup>, Atsushi ONO<sup>1</sup>, Toshikazu MIYAGISHIMA<sup>1</sup>,  
Taku NAGAO<sup>3</sup> and Tetsuro URUSHIDANI<sup>1,2</sup>

<sup>1</sup>Toxicogenomics Project, National Institute of Biomedical Innovation,  
7-6-8 Asagi, Ibaraki, Osaka 567-0085, Japan

<sup>2</sup>Department of Pathophysiology, Faculty of Pharmaceutical Sciences,  
Doshisha Women's College of Liberal Arts, Kodo, Kyotanabe, Kyoto 610-0395, Japan

<sup>3</sup>National Institute of Health Sciences, 1-18-1 Kamiyoga, Setagaya-Ku, Tokyo 158-8501, Japan

(Received August 17, 2007; Accepted August 27, 2007)

**ABSTRACT** — To identify candidate biomarker gene sets to evaluate the potential risk of chemical-induced glutathione depletion in livers, we conducted microarray analysis on rat livers administered with phorone (40, 120 and 400 mg/kg), a prototypical glutathione depletor. Hepatic glutathione content was measured and glutathione depletion-responsive gene probe sets (GSH probe sets) were identified using Affymetrix Rat Genome 230 2.0 GeneChip by the following procedure. First, probe sets, whose signal values were inversely correlated with hepatic glutathione content throughout the experimental period, were statistically identified. Next, probe sets, whose average signal values were greater than 1.5-fold compared to those of controls 3 hr after phorone treatment, were selected. Finally, probe sets without unique Entrez Gene ID were removed, ending up with 161 probe sets in total. The usefulness of the identified GSH probe sets was verified by a toxicogenomics database. It was shown that signal profiles of the GSH probe sets in rats treated with bromobenzene were strongly altered compared with other chemicals. Focusing on bromobenzene, time-course profiles of hepatic glutathione content and gene expression revealed that the change in gene expression profile was marked after the bromobenzene treatment, whereas hepatic glutathione content had recovered after initial acute depletion, suggesting that the gene expression profile did not reflect the hepatic glutathione content itself, but rather reflects a perturbation of glutathione homeostasis. The identified GSH probe sets would be useful for detecting glutathione-depleting risk of chemicals from microarray data.

**KEY WORDS:** Glutathione, Rat, Liver, Microarray, Toxicity, Toxicogenomics, Phorone

### INTRODUCTION

Microarray analysis displays tens of thousands of nucleotide probes on a substrate surface, and enables the measurement of mRNA levels of large numbers of genes simultaneously (Rockett and Dix, 2000). Microarray analysis is aimed at toxicological investigation and is called toxicogenomics (Boverhof and Zacharewski, 2006). This is thought to be useful for such points as: I) understanding the molecular mechanisms of toxicity, II) the early prediction of drug toxic-

ity risk, and III) improvement in extrapolation of experimental animal data to humans (Orphanides, 2003). At present, the liver is one of the most favored target organs in Toxicogenomics studies for the following reasons: 1) it is exposed to relatively higher levels of administered drugs, 2) it is a relatively homogenous organ and thus easy to sample, and 3) it can dramatically affect the pharmac/toxico-kinetics of the drugs in the body by the first-pass effect (Parkinson, 2001). Furthermore, hepatotoxicity has been a critical concern in drug development (Kaplowitz, 2004; Li, 2002).

These issues have motivated toxicologists to investigate liver toxicity using the toxicogenomics technique.

The Toxicogenomics Project in Japan (TGP; <http://www.tgp.nibio.go.jp/index-e.html>) has been completed by the National Institute of Health Sciences and 17 pharmaceutical companies after 5 years' collaboration from 2002 (Urushidani and Nagao, 2005; Takashima *et al.*, 2006). In the project, five rats per group were administered with toxicological prototype drugs once daily, where three dose-ranges were set, and liver samples were collected 3, 6, 9 and 24 hr after a single treatment, as well as 4, 9, 15 and 29 days after repetitive treatment. Of the collected liver samples, three samples per group were subjected to microarray analysis using the Affymetrix GeneChip system. In addition, toxicological data, such as blood chemistry and histopathology, were collected simultaneously. Such a large-scale database would be invaluable for scientists not only as a reference database but also as a resource for screening candidate toxicogenomic biomarker sets.

Glutathione serves vital functions in detoxifying electrophiles and scavenging free radicals (Lu, 1999), and hepatotoxicity caused by glutathione depletion has been intensely investigated. In the case of acetaminophen overdose, acetaminophen is metabolically activated by phase I drug metabolizing enzymes to form a reactive metabolite, *N*-acetyl-*p*-benzoquinone imine (NAPQI), which covalently binds to proteins (Dahlin *et al.*, 1984; James *et al.*, 2003). Although NAPQI can be detoxified by glutathione conjugation under ordinary conditions, an excess dose of acetaminophen depletes 90% of hepatic glutathione, and reactive NAPQI forms protein adducts (Mitchell *et al.*, 1973; James *et al.*, 2003), resulting in hepatocyte necrosis.

Previously, sixty-nine gene probe sets of Rat Genome U34A GeneChip (Affymetrix, Inc.) were identified as glutathione depletion-responsive genes, using L-buthionine-(S,R)-sulfoximine (BSO) as a glutathione-depleting agent (Kiyosawa *et al.*, 2004). Although the probe sets were thought to be useful for evaluation of drug-induced glutathione deficiency in rat liver, the study had two major drawbacks. First, the sample size used for the study was relatively small: one dose setting and one time point of observation, using 4 rats per group. Secondly, BSO depletes hepatic glutathione by inhibiting  $\gamma$ -glutamylcysteine synthetase, a key enzyme of glutathione synthesis (Moinova and Mulcahy, 1999). In the case of acetaminophen-induced glutathione depletion, an overdose of acetaminophen

depletes hepatic glutathione by extended conjugation of glutathione with activated metabolites such as NAPQI. Therefore, BSO-induced glutathione depletion would probably not appropriately reflect the drug-induced one. For these reasons, an alternative glutathione-depleting model, other than the BSO model, would be useful for better explaining drug-induced glutathione depletion, in view of the gene expression profile.

Phorone is an  $\alpha$ ,  $\beta$ -unsaturated compound, which strongly depletes hepatic glutathione content by conjugation with glutathione, by action of glutathione *S*-transferase (GST), and is excreted from liver (Boyland and Chasseaud, 1967; van Doorn *et al.*, 1978). Comparing the glutathione-depleting mechanism of phorone with that of BSO, the phorone-induced glutathione depletion mechanism is thought to be more similar to that induced by acetaminophen overdosing, where activated metabolites such as NAPQI deplete glutathione by being conjugated with glutathione and then are excreted from liver.

In this paper, we present candidate biomarker probe sets of RAE 230A GeneChip for evaluation of the potential risk of drug-induced glutathione depletion in rat livers, using phorone as a glutathione-depleting agent. The toxicological significance of identified biomarker probe sets was examined using a large-scale TGP database.

## MATERIALS AND METHODS

### Chemicals

Phorone, acetaminophen, thioacetamide, phenylbutazone, glibenclamide, methapyrilene hydrochloride and perhexiline maleate were purchased from Sigma-Aldrich (St. Louis, MO, USA). Clofibrate, aspirin and chlorpromazine were purchased from Wako Pure Chemical Industries (Osaka, Japan). Bromobenzene, hexachlorobenzene, carbon tetrachloride and coumarin were purchased from Tokyo Chemical Industry (Tokyo, Japan).

### Animal treatment

Six-week old-male Crj:CD(SD)IGS rats (Charles River Japan, Kanagawa, Japan) were used in the study. The animals were individually housed in stainless-steel cages in a room that was lighted for 12 hr (7:00-19:00) daily, ventilated with an air-exchange rate of 15 times per hour, and maintained at 21-25°C with a relative humidity of 40-70%. Each animal was allowed free access to water and pellet food (CRF-1, sterilized by

## Glutathione-depletion responsive genes in rat liver.

radiation, Oriental Yeast Co., Japan). Five rats per group were administered with phorone (40, 120 or 400 mg/kg, i.p.). Five rats per group were administered orally with acetaminophen (1000 mg/kg), bromobenzene (300 mg/kg), clofibrate (300 mg/kg), chlorpromazine (45 mg/kg), glibenclamide (1000 mg/kg), methapyrilene (100 mg/kg), phenylbutazone (200 mg/kg), aspirin (450 mg/kg), carbon tetrachloride (300 mg/kg), coumarin (150 mg/kg), hexachlorobenzene (300 mg/kg), perhexiline maleate (150 mg/kg) or thioacetamide (45 mg/kg). Blood samples were collected in tubes containing heparin lithium 3, 6, 9, or 24 hr after treatment for biochemical assay. The animals were then euthanized and the liver was removed and soaked in *RNAlater* (Ambion, Austin, TX, USA) immediately after sampling and stored at  $-80^{\circ}\text{C}$  until use for gene expression analysis. In the animals treated with phorone or bromobenzene, another aliquot of liver sample was immediately frozen in liquid nitrogen for measurement of hepatic glutathione contents. The remaining liver samples were then removed and fixed in 10% neutral buffered formalin for histopathological examination. The experimental protocol was reviewed and approved by the Ethics Review Committee for Animal Experimentation of the National Institute of Health Sciences.

#### Plasma biochemistry

Activities of alanine aminotransferase (ALT) and aspartate aminotransferase (AST) in plasma were determined using a 7080 Clinical Analyzer (Hitachi High-Technologies Corporation, Tokyo, Japan).

#### Histopathology

The fixed samples were dehydrated through graded alcohols and embedded in paraffin. Serial sections 2-3  $\mu\text{m}$  thick were stained with hematoxylin and eosin for pathological examination.

#### Measurement of hepatic glutathione content

The liver samples (0.1 g) were homogenized with 5% 5-sulfosalicylic acid (Sigma-Aldrich) and centrifuged at 12,000 rpm for 10 min at  $4^{\circ}\text{C}$ . The supernatant was used for the measurement of total glutathione content in the liver using the Total Glutathione Quantification Kit (Dojindo Laboratories), according to the manufacturer's instructions.

#### Microarray analysis

Liver samples were homogenized with RLT buffer, supplied in the RNeasy Mini Kit (Qiagen,

Valencia, CA, USA), using Mill Mixer (Qiagen) and zirconium beads. Total RNA was isolated using Bio Robot 3000 (Qiagen). DNase I treatment was performed using RNase-Free DNase set (Qiagen) for 15 min at room temperature. GeneChip analysis was performed on 3 out of 5 samples in each group according to the Affymetrix standard protocol. Briefly, a total of RNA of 5  $\mu\text{g}$  prepared from the individual rat liver samples was used for cDNA synthesis using the T7-(dT)<sub>24</sub> primer (Affymetrix) and Superscript Choice System (Invitrogen, Carlsbad, CA, USA). The cDNA was purified using cDNA Cleanup Module (Affymetrix), and biotin-labeled cRNA mix was transcribed using the BioArray High Yield RNA Transcription Labeling Kit (Enzo Diagnostics, Farmingdale, NY, USA). Ten micrograms of fragmented cRNA cocktails were hybridized to the RAE 230A GeneChip array for all samples except for that of phorone- and corresponding vehicle-treated rats, which were hybridized to the RAE 230 2.0 array for 18 hr at  $45^{\circ}\text{C}$  at 60 rpm. GeneChip was washed and stained using Fluidics Station 400 (Affymetrix) according to the Affymetrix standard protocol and scanned using Gene Array Scanner (Affymetrix). The scanned data images were digitalized using Affymetrix Microarray Suite ver. 5.0 (Affymetrix), and the data was scaled by adjusting the mean Signal value to 500.

#### Microarray data analysis

We primarily use global mean normalization for data analysis in our project. Firstly, using vehicle- and phorone (40 and 120 mg/kg)-treated rats, where the total number of rats was 36, both Spearman's and Pearson's correlation coefficients between the signal value and hepatic glutathione content were calculated for all the probe sets that existed on the RAE 230A array. The probe sets with both Spearman's coefficients and Pearson's coefficients less than -0.329 were chosen as statistically significant inverse correlations ( $N=36$ ,  $p < 0.05$ ). Secondly, probe sets, whose average signal values in 120 mg/kg phorone-treated rats at 3 h were above 1.5 compared to those of corresponding controls were selected. Then, probe sets, whose detection calls determined by Microarray Suite ver. 5.0 were all present 3 hr after phorone treatment, were selected. Finally, annotation for each probe set was obtained using NetAffx Website (Liu *et al.*, 2003), and probe sets without unique Entrez Gene ID were excluded from the analysis. For each probe set, the signal data was z-score normalized in the vehicle- and phorone (40, 120 and 400 mg/kg)-treated group. All the z-score

normalized signal data were presented as a heat map and z-score normalized glutathione content data was also presented as a heat map.

#### Statistical analysis

Dunnett's test was performed for serum chemistry and glutathione content data (between phorone-treated rat groups and vehicle-treated group at the same time point), using R software ([www.r-project.org](http://www.r-project.org)). Serum chemistry data (other than that of phorone-treated rats) was analyzed by F-test to evaluate the homogeneity of variance. If the variance was homogeneous, Student's *t*-test was applied. If the variance was heterogeneous, Aspin-Welch's *t*-test was performed (Snedecor and Cochran, 1989). F-test, Student's *t*-test and Aspin-Welch's *t*-test were performed using Microsoft Excel 2007. Both Spearman's and Pearson's correlation coefficients were calculated using Microsoft Excel 2007. A p-value of < 0.05 was considered statistically significant. Principal component analysis (PCA) was performed using the Spotfire Functional Genomics Package ver. 17.4.832 (Spotfire, Somerville, MA, USA).

## RESULTS

#### Plasma biochemistry in phorone-treated rats

There were no apparent fluctuations of plasma ALT activity in 40 and 120 mg/kg phorone-treated rats throughout the experimental period (Fig. 1). Plasma ALT activity was obviously elevated in rats 24 hr after 400 mg/kg phorone treatment.

#### Glutathione content in phorone-treated rat liver

Hepatic glutathione content was significantly decreased 3, 6 and 9 hr for 40 mg/kg phorone-treated rats, and recovered above the control level 24 hr after treatment (Fig. 2). Hepatic glutathione content was significantly decreased to an 8.3-fold lower level compared with the control 3 hr after the 120 mg/kg phorone-treated rats, and gradually recovered 6 and 9 hr after treatment, resulting in a 1.52-fold higher level compared with control 24 hr after treatment. Hepatic glutathione content was significantly decreased to a 22- to 30-fold lower level compared with control 3, 6 and 9 hr after the 400 mg/kg phorone-treated rats, and recovered to the control level 24 hr after treatment.

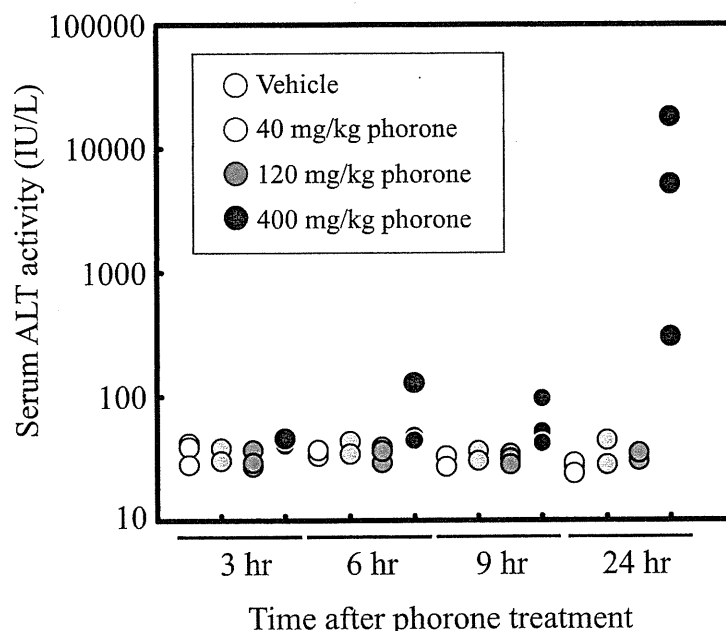


Fig. 1. Activity of alanine aminotransferase in plasma. Each dot represents the value of an individual animal.

### Identification of glutathione deficiency-correlated gene probe sets

A hundred and sixty-one probe sets were identified as glutathione deficiency-correlated gene probe sets, or GSH probe sets (Table 1), and classified to 5 groups, i.e., “antioxidant, phase II drug metabolizing enzymes, and oxidative stress markers” (11 probe sets), “transporter” (13 probe sets), “metabolism” (20 probe sets), “transcription factors and signal transduction-related, and protein turnover-related genes” (79 probe sets), and “miscellaneous” (37 probe sets). Both the z-score transformed hepatic glutathione content and z-score transformed signal levels of the GSH probe sets are presented as a heat map (Fig. 3). PCR primers and TaqMan probes for 4 genes from the list above, namely tribbles homolog 3 (accession no. AB020967), heme oxygenase-1 (NM\_012580), thioredoxin reductase-1 (NM\_031614) and  $\gamma$ -glutamylcysteine synthetase modifier subunit (NM\_017305), were synthesized and quantitative RT-PCR was performed using

the TaqMan Universal PCR Master Mix (Applied Biosystems), and the mRNA level was quantified with a GeneAmp 5700 Sequence Detection System (Applied Biosystems) according to the manufacturer’s instructions. It was confirmed that quantification by GeneChip was sufficient (data not shown).

### Plasma biochemistry and histopathological findings in rat liver treated with various hepatotoxicants

Rats treated with bromobenzene, methapyrilene or thioacetamide showed significant increase in plasma ALT activity 24 hr after treatment (Table 2). Rats treated with acetaminophen, chlorpromazine, glibenclamide or methapyrilene showed significant increase in serum AST activity 24 hr after treatment. Rats treated with acetaminophen, bromobenzene, methapyrilene, carbon tetrachloride, coumarin or thioacetamide showed histopathological changes 24 hr after treatment, while rats treated with clofibrate, chlorpromazine, glibenclamide, phenylbutazone, aspirin,

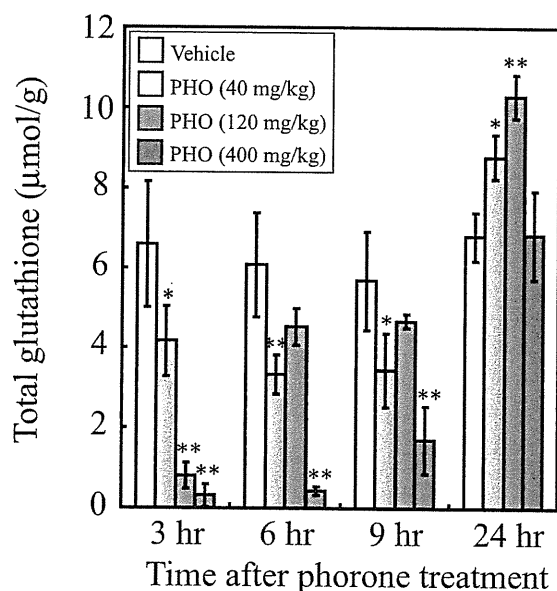


**Fig. 2.** Hepatic glutathione content after phorone treatment.

Three rats per group were treated with 40, 120 or 400 mg/kg phorone or vehicle, and the livers were removed 3, 6, 9 and 24 hr after treatment. Hepatic glutathione content (total) was measured and the data are presented as mean  $\pm$  S.D. \*\* and \*,  $p < 0.01$  and  $p < 0.05$  by Dunnett’s test, respectively.



**Table 1.** Glutathione depletion-responsive gene probe sets (GSH probe sets).

Affymetrix probe ID	Correlation coefficient		Gene Symbol	Annotation
	Spearman's	Pearson's		
<b>Antioxidant, phase II drug-metabolizing enzymes and oxidative stress markers</b>				
1368037_at	-0.602	-0.368	Cbr1	carbonyl reductase 1
1387221_at	-0.720	-0.712	Gch	GTP cyclohydrolase 1
1368503_at	-0.702	-0.650	Gch	GTP cyclohydrolase 1
1370030_at	-0.570	-0.448	Gclm	glutamate cysteine ligase, modifier subunit
1370080_at	-0.611	-0.609	Hmox1	heme oxygenase (decycling) 1
1387282_at	-0.680	-0.589	Hspb8	heat shock 22kDa protein 8
1388721_at	-0.747	-0.660	Hspb8	heat shock 22kDa protein 8
1389578_at	-0.649	-0.582	Isrip	ischemia/reperfusion inducible protein
1372510_at	-0.589	-0.578	Srxn1	Sulfiredoxin 1 homolog ( <i>S. cerevisiae</i> )
1398791_at	-0.600	-0.471	Txnrd1	thioredoxin reductase 1
1386958_at	-0.666	-0.459	Txnrd1	thioredoxin reductase 1
<b>Transporter</b>				
1374423_at	-0.711	-0.688	Hiat1_predicted	hippocampus abundant gene transcript 1 (predicted)
1370934_at	-0.656	-0.579	Nup153	nucleoporin 153
1367803_at	-0.430	-0.523	Nup54	nucleoporin 54
1371754_at	-0.330	-0.497	Slc25a25	solute carrier family 25 (mitochondrial carrier, phosphate carrier), member 25
1369099_at	-0.356	-0.567	Slc30a1	solute carrier family 30 (zinc transporter), member 1
1370286_at	-0.858	-0.813	Slc38a2	solute carrier family 38, member 2
1398771_at	-0.651	-0.520	Slc3a2	solute carrier family 3 (activators of dibasic and neutral amino acid transport), member 2
1387130_at	-0.726	-0.455	Slc40a1	solute carrier family 39 (iron-regulated transporter), member 1
1387693_a_at	-0.731	-0.601	Slc6a9	solute carrier family 6 (neurotransmitter transporter, glycine), member 9
1369772_at	-0.609	-0.473	Slc6a9	solute carrier family 6 (neurotransmitter transporter, glycine), member 9
1373787_at	-0.619	-0.513	Slc6a9	solute carrier family 6 (neurotransmitter transporter, glycine), member 9
1368391_at	-0.780	-0.700	Slc7a1	solute carrier family 7 (cationic amino acid transporter, y <sup>+</sup> system), member 1
1368392_at	-0.591	-0.626	Slc7a1	solute carrier family 7 (cationic amino acid transporter, y <sup>+</sup> system), member 1
<b>Metabolism</b>				
1387925_at	-0.747	-0.574	Asns	asparagine synthetase
1386928_at	-0.352	-0.409	Bcat2	branched chain aminotransferase 2, mitochondrial
1374034_at	-0.762	-0.756	Cars_predicted	cysteinyl-tRNA synthetase (predicted)
1368709_at	-0.537	-0.492	Fut1	fucosyltransferase 1
1375852_at	-0.441	-0.532	Hmgcr	3-hydroxy-3-methylglutaryl-Coenzyme A reductase
1387848_at	-0.413	-0.500	Hmgcr	3-hydroxy-3-methylglutaryl-Coenzyme A reductase
1376418_a_at	-0.679	-0.549	Iars_predicted	isoleucine-tRNA synthetase (predicted)

## Glutathione-depletion responsive genes in rat liver.

**Table 1.** Continued.

Affymetrix probe ID	Correlation coefficient		Gene Symbol	Annotation
	Spearman's	Pearson's		
1389551_at	-0.373	-0.359	Lactb2	lactamase, beta 2
1371350_at	-0.773	-0.683	LOC683283	similar to S-adenosylmethionine synthetase isoform type-2 (Methionine adenosyltransferase 2) (AdoMet synthetase 2) (Methionine adenosyltransferase II) (MAT-II)
1377287_at	-0.495	-0.532	Mars2_predicted	methionine-tRNA synthetase 2 (mitochondrial) (predicted)
1375684_at	-0.554	-0.490	Neu1	neuraminidase 1
1367811_at	-0.675	-0.459	Phgdh	3-phosphoglycerate dehydrogenase
1369785_at	-0.754	-0.691	Ppat	phosphoribosyl pyrophosphate amidotransferase
1388756_at	-0.614	-0.529	Ppcs	phosphopantothencycysteine synthetase
1372665_at	-0.682	-0.633	Psat1	phosphoserine aminotransferase 1
1375964_at	-0.641	-0.615	Psph	phosphoserine phosphatase
1388521_at	-0.428	-0.544	Pycs_predicted	pyrroline-5-carboxylate synthetase (glutamate gamma-semialdehyde synthetase) (predicted)
1372602_at	-0.490	-0.460	RGD1311800	similar to genethonin 1
1398452_at	-0.421	-0.431	RGD1559923_predicted	similar to chromosome 14 open reading frame 35 (predicted)
1372009_at	-0.569	-0.478	Yars	tyrosyl-tRNA synthetase

**Transcription factor, signal transduction-related and protein turnover-related gene**

1388179_at	-0.370	-0.379	Acvr2b	activin receptor IIB
1369146_a_at	-0.433	-0.479	Ahr	aryl hydrocarbon receptor
1378140_at	-0.600	-0.606	Arl11	ADP-ribosylation factor-like 11
1367960_at	-0.470	-0.485	Arl4a	ADP-ribosylation factor-like 4A
1389623_at	-0.605	-0.623	Atf1	activating transcription factor 1
1375941_at	-0.594	-0.513	Baiap211	BAlI-associated protein 2-like 1
1374947_at	-0.584	-0.567	Bcar3_predicted	breast cancer anti-estrogen resistance 3 (predicted)
1376754_at	-0.771	-0.740	Cars_predicted	cysteinyl-tRNA synthetase (predicted)
1391572_at	-0.804	-0.802	Cars_predicted	cysteinyl-tRNA synthetase (predicted)
1387087_at	-0.720	-0.734	Cebpb	CCAAT/enhancer binding protein (C/EBP), beta
1387244_at	-0.504	-0.371	Cgrrf1	cell growth regulator with ring finger domain 1
1372498_at	-0.626	-0.608	Ciapin1	cytokine induced apoptosis inhibitor 1
1399141_at	-0.640	-0.664	Clk4	CDC like kinase 4
1376811_a_at	-0.571	-0.534	Cpsf6_predicted	cleavage and polyadenylation specific factor 6, 68kDa (predicted)
1369737_at	-0.558	-0.614	Creml	cAMP responsive element modulator
1370979_at	-0.433	-0.475	Ddx20	DEAD/H (Asp-Glu-Ala-Asp/His) box polypeptide 20, 103kD
1375901_at	-0.497	-0.360	Ddx21a	DEAD (Asp-Glu-Ala-Asp) box polypeptide 21a
1373200_at	-0.581	-0.505	Eef1e1_predicted	eukaryotic translation elongation factor 1 epsilon 1 (predicted)

**Table 1.** Continued.

Affymetrix probe ID	Correlation coefficient		Gene Symbol	Annotation
	Spearman's	Pearson's		
1368967_at	-0.629	-0.484	Eif2b3	eukaryotic translation initiation factor 2B, subunit 3 gamma
1386888_at	-0.794	-0.776	Eif4ebp1	eukaryotic translation initiation factor 4E binding protein 1
1388666_at	-0.581	-0.588	Enc1	ectodermal-neural cortex 1
1382059_at	-0.593	-0.634	Fbxo30	F-box protein 30
1372526_at	-0.675	-0.776	Flcn	folliculin
1374530_at	-0.671	-0.601	Fzd7_predicted	frizzled homolog 7 ( <i>Drosophila</i> ) (predicted)
1373499_at	-0.731	-0.622	Gas5	growth arrest specific 5
1388953_at	-0.682	-0.665	Gnl3	guanine nucleotide binding protein-like 3 (nucleolar)
1373094_at	-0.788	-0.587	Gtf2h1_predicted	general transcription factor II H, polypeptide 1 (predicted)
1367741_at	-0.618	-0.579	Herpud1	homocysteine-inducible, endoplasmic reticulum stress-inducible, ubiquitin-like domain member 1
1372693_at	-0.462	-0.559	Hnrpa1	heterogeneous nuclear ribonucleoprotein A1
1387430_at	-0.754	-0.774	Hsf2	heat shock factor 2
1388587_at	-0.571	-0.636	Ier3	immediate early response 3
1367795_at	-0.666	-0.597	Ifrd1	interferon-related developmental regulator 1
1368160_at	-0.644	-0.700	Igfbp1	insulin-like growth factor binding protein 1
1387440_at	-0.432	-0.330	Ireb2	iron responsive element binding protein 2
1373374_at	-0.813	-0.812	Lmo4	LIM domain only 4
1373303_at	-0.339	-0.409	LOC312030	similar to splicing factor, arginine/serine-rich 2, interacting protein
1374154_at	-0.762	-0.677	LOC312030	Similar to splicing factor, arginine/serine-rich 2, interacting protein
1374857_at	-0.555	-0.445	LOC499709	similar to nucleolar protein family A, member 1
1373133_at	-0.630	-0.692	LOC500282	similar to ADP-ribosylation factor-like 10C
1368874_a_at	-0.775	-0.801	Mafg	v-maf musculoaponeurotic fibrosarcoma oncogene family, protein G (avian)
1368273_at	-0.342	-0.453	Mapk6	mitogen-activated protein kinase 6
1384427_at	-0.766	-0.764	Mdm2_predicted	transformed mouse 3T3 cell double minute 2 homolog (mouse) (predicted)
1388990_at	-0.544	-0.492	Mki67ip	Mki67 (FHA domain) interacting nucleolar phosphoprotein
1375442_at	-0.670	-0.696	Mphosph10_predicted	M-phase phosphoprotein 10 (U3 small nucleolar ribonucleoprotein) (predicted)
1368308_at	-0.513	-0.622	Myc	myelocytomatosis viral oncogene homolog (avian)
1374437_at	-0.717	-0.665	Nars	asparaginyl-tRNA synthetase
1376704_a_at	-0.577	-0.485	Ndn12	needin-like 2
1389996_at	-0.645	-0.657	Nek1_predicted	NIMA (never in mitosis gene a)-related expressed kinase 1 (predicted)
1389765_at	-0.564	-0.579	Nle1_predicted	notchless homolog 1 ( <i>Drosophila</i> ) (predicted)
1368173_at	-0.444	-0.403	Nol5	nucleolar protein 5
1368032_at	-0.451	-0.365	Nolc1	nucleolar and coiled-body phosphoprotein 1
1387152_at	-0.375	-0.508	Nrbf2	nuclear receptor binding factor 2

## Glutathione-depletion responsive genes in rat liver.

**Table 1.** Continued.

Affymetrix probe ID	Correlation coefficient		Gene Symbol	Annotation
	Spearman's	Pearson's		
1368068_a_at	-0.605	-0.488	Pacsin2	protein kinase C and casein kinase substrate in neurons 2
1372857_at	-0.720	-0.706	Pacsin2	protein kinase C and casein kinase substrate in neurons 2
1374326_at	-0.576	-0.544	Ppan	peter pan homolog (Drosophila)
1369104_at	-0.618	-0.554	Prkaa1	protein kinase, AMP-activated, alpha 1 catalytic subunit
1368087_a_at	-0.419	-0.407	Ptpn21	protein tyrosine phosphatase, non-receptor type 21
1371081_at	-0.740	-0.765	Rapgef4	Rap guanine nucleotide exchange factor (GEF) 4
1374750_at	-0.773	-0.799	Rapgef6_predicted	Rap guanine nucleotide exchange factor (GEF) 6 (predicted)
1388522_at	-0.689	-0.713	RGD1310383_predicted	similar to T-cell activation protein phosphatase 2C (predicted)
1374945_at	-0.587	-0.463	RGD1359191	GCD14/PCMT domain containing protein RGD1359191
1373075_at	-0.762	-0.664	RGD1560888_predicted	similar to Cell division protein kinase 8 (Protein kinase K35) (predicted)
1372062_at	-0.703	-0.708	RGD1563395_predicted	similar to cyclin-dependent kinase 2-interacting protein (predicted)
1371517_at	-0.660	-0.627	RGD1566234_predicted	similar to Grb10 protein (predicted)
1377503_at	-0.558	-0.606	Riok2	RIO kinase 2 (yeast)
1387201_at	-0.766	-0.774	Rnf138	ring finger protein 138
1389258_at	-0.592	-0.653	Rnf138	ring finger protein 138
1376440_at	-0.741	-0.715	Rnf139_predicted	ring finger protein 139 (predicted)
1398572_at	-0.670	-0.547	Rnmt	RNA (guanine-7-) methyltransferase
1376065_at	-0.662	-0.617	Rrs1_predicted	RRS1 ribosome biogenesis regulator homolog (S. cerevisiae) (predicted)
1375441_at	-0.724	-0.680	Sars1	seryl-aminoacyl-tRNA synthetase 1
1374864_at	-0.370	-0.339	Spry2	sprouty homolog 2 (Drosophila)
1388967_at	-0.744	-0.714	Tefe3_predicted	transcription factor E3 (predicted)
1388780_at	-0.683	-0.681	Terf2ip	telomeric repeat binding factor 2, interacting protein
1387450_at	-0.695	-0.708	Tgfa	transforming growth factor alpha
1370694_at	-0.858	-0.760	Trib3	tribbles homolog 3 (Drosophila)
1386321_s_at	-0.835	-0.676	Trib3	tribbles homolog 3 (Drosophila)
1370695_s_at	-0.831	-0.701	Trib3	tribbles homolog 3 (Drosophila)
1388868_at	-0.779	-0.736	Zfp216_predicted	zinc finger protein 216 (predicted)
<b>Miscellaneous</b>				
1385616_a_at	-0.734	-0.557	Asf1a_predicted	ASF1 anti-silencing function 1 homolog A (S. cerevisiae) (predicted)
1389569_at	-0.647	-0.578	Bxdc2	brix domain containing 2
1373196_at	-0.378	-0.414	Efha2	EF hand domain family, member A2
1372873_at	-0.599	-0.673	Fbxo38_predicted	F-box protein 38 (predicted)
1373836_at	-0.412	-0.503	Fytd1	Forty-two-three domain containing 1
1374043_at	-0.379	-0.444	Gramd3	GRAM domain containing 3